11-1995

A focused ion beam secondary ion mass spectrometry system

G. A. Crow

Locke Christman

Mark Utlaut
University of Portland, utlaut@up.edu

A focused ion beam secondary ion mass spectroscopy system

G. A. Crow
Intel Corporation, 5200 N. E. Elam Young Parkway, Hillsboro, Oregon 97124

Locke Christman
FEI Co., 7451 N. E. Evergreen Parkway, Hillsboro, Oregon 97124

M. Utlaut
Department of Physics, University of Portland, Portland, Oregon 97203

(Received 2 June 1995; accepted 24 August 1995)

This article describes a Ga^+ focused ion beam secondary ion mass spectroscopy system, and measures several quantities of interest to aid in interpreting secondary ion mass spectroscopy results. We have measured sputter yields and rates, estimated the instrument efficiency, and calculated useful yields and practical sensitivities for a variety of elements used in the semiconductor industry. We have performed measurements at the system base pressure, and have also introduced oxygen and iodine to determine any enhancement effects. © *1995 American Vacuum Society.*

I. INTRODUCTION

Improvements in analytic techniques for process evaluation, failure analysis, and integrated circuit (IC) modification are necessary as miniaturization of semiconductor microstructures continues to progress. Often both visual and chemical characterizations are necessary at high spatial lateral and vertical resolution. The use of focused ion beams (FIBs) for preparing cross sections[1] and transmission electron microscopy (TEM) samples,[2] depositing metals and insulators,[3] and selectively etching metals and insulators[4] is well documented. Chemical characterization with FIB is less well known, but FIB combined with secondary ion mass spectroscopy (SIMS) makes possible high lateral resolution chemical maps, depth profiling, and spectral analysis from small areas. Levi-Setti *et al.*[5–7] have shown the usefulness of high spatial resolution chemical maps in a variety of biological and materials investigations, and Crow[8] has shown the utility of chemical mapping, depth profiling, and spectral analysis in the semiconductor field. Even though there is a trade off between lateral spatial resolution and detected elemental sensitivity (due to the limited volume of material being analyzed within the beam at any time), FIB/SIMS can have greater sensitivity than electron beam analytical instruments in many cases.[9]

Since SIMS is a destructive analytical technique, using a FIB with SIMS in one instrument allows high lateral spatial resolution chemical information to be obtained at the cost of partly or wholly destroying the sample. However, one can exploit the destruction in order to obtain one-, two-, or three-dimensional chemical maps.

One of the major limitations of SIMS is that quantification is at best difficult. Matrix effects and the presence of oxides can influence dramatically the yields.[10] In order to interpret spectra, depth profiles, and chemical maps, it is necessary to know the sputter yields and rates, ionization yields, and sensitivities for the materials of interest.

Much data and theory have been published for conventional SIMS, but only recently has work begun in measuring quantities of interest for the semiconductor industry. Benninghoven *et al.*[10] have compiled data about SIMS, but there is little known about Ga^+ beams. Ga is used almost exclusively in FIB because of its ease of manufacture, high brightness, long life, and high stability. Recently, Leslie[11] has published the first attempt at measuring and compiling quantities of interest for use with FIB/SIMS. We have undertaken an initial similar though more limited study of pure elements of interest to the semiconductor industry, in order to better quantify the role of FIB/SIMS.

II. THE SYSTEM

The FIB system used to obtain data was an FEI FIB611 with SIMS map option.[12] The system employs a Ga^+ liquid metal ion source, a two lens focusing column, and operates at beam voltages between 5 and 25 keV. A variable aperture system allows beam sizes from 30 to 350 nm with beam currents of 16 pA–10 nA.

The SIMS consists of a movable secondary ion transfer optics section which conveys secondary ions into a radio-frequency (rf) quadrupole mass spectrometer. Mass filtered ions are detected with an on-axis channel electron multiplier (CEM). The "SIMS head" is easily, mechanically moved into and out of position by a rack and pinion system with mechanical stops.[13]

A schematic transverse cross section of the transfer optics is shown in Fig. 1. Secondary ions are extracted from the sample surface by a tilted extraction plate (±200 V) into an electrostatic spherical ($r=9$ mm) analyzer (through which the primary Ga^+ beam also passes via a hole in the outer sphere segment). The energy filtered ions are brought to a focus in the object plane of the electrostatic lens system, and conveyed to the input aperture of the quadrupole filter. Figure 2 shows typical trajectories for $M=27$ ions.[14] The polarity of the extractor, analyzer, lens, and detector are software switchable so either positive or negative secondary ions can be collected. The quadrupole mass filter is a flange mounted Extrel[15] with 19 mm rods. Mass scans are performed in the constant resolution mode with mass resolution of 0.7 amu. The tilted extractor plate was chosen as a compromise for viewing both samples at normal incidence, and the tilted faces of cross-sectioned samples.

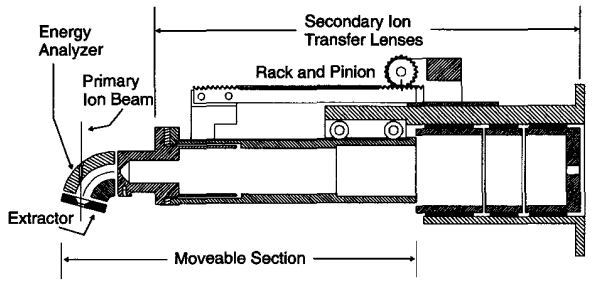

FIG. 1. A transverse cross-sectional view of the SIMS transport optics. The pinion gear is externally driven.

The electronics for the SIMS consists of an optics controller which provides programmable differential voltage sources for extraction potential, energy passband, and mass filter entry angle and energy, in addition to detector control voltages and interlock facilities. Pulses from the CEM detector in the mass filter are passed to a preamplifier and then into a high speed (20 MHz) 24 bit software controlled count engine. A SIMS distributed processor (486 CPU) is controlled through an Ethernet communications link, and all SIMS control is handled from the main FIB computer operating in the Windows environment, using custom integrated FIB/SIMS software. This allows high speed counting.

III. USEFUL CHARACTERIZATION

There exists a vast amount of data and theory for conventional SIMS (see Ref. 10). To facilitate a comparison of instrumental performance and to better understand fundamental physical processes occurring, there are several useful quantities which we have undertaken to measure. We have done these measurements at the system base pressure (2×10^{-7} Torr) and also by flooding the sample with oxygen or iodine in order to determine the effects on sputter and ionization yield. Quantities of importance are

(1) the *sputter yield and sputter rate* which are the number of sputtered sample atoms per incident primary ion and the sputtered volume per unit primary current,
(2) *secondary ion yield*, which is the number of secondary ions generated per incident primary ion,
(3) *practical sensitivity*, which is the secondary ion count rate per unit incident beam current, and
(4) the *useful yield*, which is the number of detected secondary ions per total sputtered particles.

For this experiment, we used a 1 nA Ga^+ primary beam at 25 keV, and collected positive secondary ions. The primary beam was first rastered over a 15×15 μm area on the selected targets to remove the native oxide. The removal of the oxide was determined by monitoring the secondary ion signal in the depth profile mode and was continued until the count rate became asymptotic. A 10×10 μm area within the precleaned area was then chosen and a crater was sputtered while monitoring in the depth profile mode. The primary beam was at normal incidence to the sample and initially the vacuum was 2×10^{-7} Torr. Each target was precleaned and a crater sputtered at this vacuum level, and then the process was repeated for the cases of turning on an oxygen jet or an iodine jet. Oxygen was delivered onto the sample through a small hole in the SIMS extraction plate and the chamber pressure was kept at 1×10^{-5} Torr. Iodine was introduced through a movable needle brought close to the area of interest, and at a nonoptimal shallow angle (15°). The chamber pressure was 8×10^{-6} Torr with the introduction of iodine. It is well known that there exist optimal angle, distance, and flux for iodine enhanced FIB sputtering. Present physical limitations precluded the optimal geometry from being used.

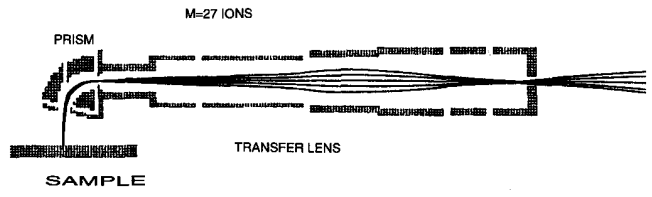

FIG. 2. Calculated trajectories through the system for $M=27$ ions using the charged particle optics simulation program SIMION (Ref. 14).

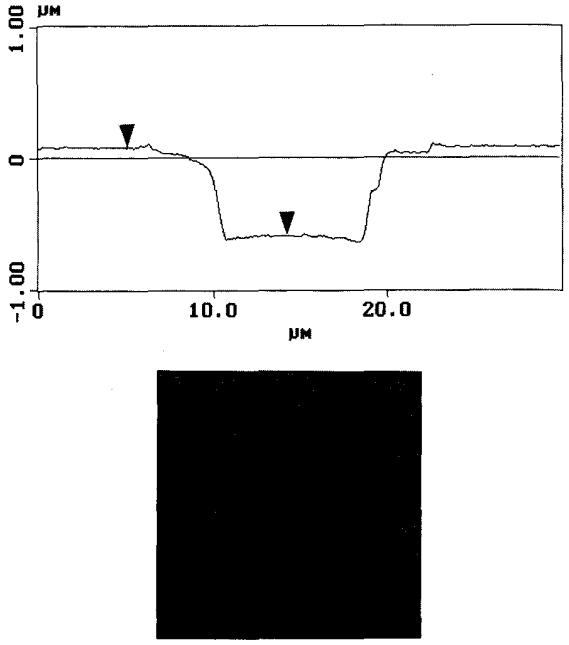

FIG. 3. Typical AFM measurements of the sputtered craters for the case of Si.

The volume of the sputtered craters was measured with a Digital Instruments atomic force microscope (AFM)[16] in the tapping mode, and confirmed with a Burleigh AFM.[17] The 10 μm$\times$10 μm sputter crater size allowed the depths to be sufficiently probed. Figure 3 shows a typical AFM measurement result.

IV. RESULTS

Table I shows the measured sputter yields and sputter rates and the enhancement due to oxygen and iodine. Leslie's[11] value are included for comparison. It is clear from the data that there is virtually no sputter enhancement from the presence of oxygen, but that there is 3×–5× enhancement with iodine in this geometry. A previous study[18] indi-

TABLE I. Measured values of sputter yield, sputter rate, and enhancement effects to the sputter yield and sputter rate for this study.

Element	Gas	Sputter yield (this study)	Sputter yield (Ref. 11)	Enhancement (this study)	Sputter rate (μm^3/nc)	Enhancement (this study)
Al	Bkgnd	2.14	2.89	NA	0.22	NA
	O	2.2	NA	1.028	0.23	1.05
	I	11.6	NA	5.43	1.2	5.45
Si	Bkgnd	1.78	2.08	NA	0.22	NA
	O	1.71	NA	0.961	0.21	0.96
	I	6.91	NA	3.88	0.86	3.91
Ti	Bkgnd	3.4	3.35	NA	0.38	NA
	O	3.5	NA	1.03	0.39	1.03
	I	14.0	NA	4.12	1.55	4.08
Mo	Bkgnd	1.41	1.32	NA	0.14	NA
	O	1.43	NA	1.01	0.14	1
	I	5.62	NA	3.99	0.55	3.93
W	Bkgnd	1.13	1.22	NA	0.11	NA
	O	1.22	NA	1.08	0.12	1.09
	I	3.44	NA	3.04	0.34	3.09

cated for 500 eV Ar^+ that the sputter rate for Al and Ti decreased by large factors (4×–8×) when the base pressure was increased to $1–2\times10^{-5}$ Torr by introducing oxygen. Presumably this effect is due to the substrate being converted to a nonvolitle oxide, which if sputtered may redeposit. This is contrary to our result, and further experiments will determine the effect. It may be that there are differences between a scanning versus fixed beam, and differences due to current density (A/cm^2 vs mA/cm^2). Another factor that may account for this difference is that the sputter craters in this study were milled with a low aspect ratio.

Table II shows the practical sensitivity and the ionization yield for the materials we measured. The practical sensitivity indicates what level of secondary signal can be expected per unit of primary current. We have found that in the elemental materials we have analyzed, count rates scale with input beam current up to detector saturation. On samples with finite volumes, the count rate will not of course continue indefinitely with time.

It is possible to estimate the transmission efficiency for the SIMS system from a knowledge of the total current to the sample. When collecting positive secondary ions, the extractor is at ~ -200 V so that electrons and negative secondary ions are mostly forced back to the sample. Since we know *a priori* the Ga^+ primary current to the sample, measuring the total current to the sample allows an estimation of the SIMS transmission factor. If I_p and I_s^+ are the Ga^+ primary beam current and the total positive secondary ion current, then approximately,

[redacted]

If only one kind of ion is collected at a time, a correction factor for existent isotopes and oxides must be used. This FIB/SIMS allows up to four different masses to be monitored simultaneously in the depth profile mode.

Table III shows useful yields calculated from our measurements. Useful yields are necessary when attempting to

TABLE II. Measured practical sensitivities.

Element	Gas	Practical sensitivity (counts per second nA)	Ionization yield (counts per incident ion)	Ionization enhancement
Al	Bkgnd	1.48×10^5	2.37×10^{-11}	NA
	O	1.6×10^6	2.56×10^{-10}	10.8
	I	1.0×10^7	1.6×10^{-9}	67.6
Si	Bkgnd	1.25×10^3	2×10^{-13}	NA
	O	7.0×10^4	1.12×10^{-11}	56.0
	I	1.31×10^5	2.1×10^{-11}	104.8
Ti	Bkgnd	4.5×10^4	7.21×10^{-12}	NA
	O	2.5×10^6	4.0×10^{-10}	59.6
	I	1.55×10^6	2.48×10^{-10}	34.4
Mo	Bkgnd	2.1×10^3	3.36×10^{-13}	NA
	O	2.0×10^5	3.2×10^{-11}	95.2
	I	7.5×10^4	1.2×10^{-11}	35.7
W	Bkgnd	5.35×10^2	8.57×10^{-14}	NA
	O	7.45×10^3	1.19×10^{-12}	13.9
	I	1.67×10^3	2.67×10^{-13}	3.1

TABLE III. Measured useful yields, enhancements of the useful yield, and the ionization yield due to oxygen or iodine. The last column gives the ratio of the ionization enhancement to sputter enhancement due to oxygen or iodine. This gives a sense of which effect is more enhanced.

Element	Gas	Useful yield	Enhancement of useful yield	Enhancement of ionization	Ratio of ionization enhancement to sputter enhancement
Al	Bkgnd	4.3×10^{-5}	NA	NA	NA
	O	4.6×10^{-4}	10.7	10.8	10.8
	I	5.4×10^{-4}	12.6	67.6	12.4
Si	Bkgnd	4.4×10^{-6}	NA	NA	NA
	O	2.6×10^{-5}	5.9	56.0	56.0
	I	1.2×10^{-5}	2.7	104.8	27.0
Ti	Bkgnd	8.3×10^{-6}	NA	NA	NA
	O	4.5×10^{-4}	54.2	59.6	59.6
	I	6.9×10^{-5}	8.3	34.4	8.4
Mo	Bkgnd	9.3×10^{-7}	NA	NA	NA
	O	8.7×10^{-5}	93.6	95.2	95.2
	I	8.3×10^{-6}	8.9	35.7	8.95
W	Bkgnd	3×10^{-7}	NA	NA	NA
	O	3.8×10^{-6}	12.7	13.9	13.9
	I	3×10^{-7}	1	3.1	1

ascertain what analytical technique should be used. The useful yield is the ratio of the detected SIMS signal for an ion to the total number of sputtered atoms, i.e.,

$$\tau_A = Y_A / S_A I_p = \gamma\eta,$$

where Y_A is the measured secondary ion yield, S_A is the secondary sputtering yield, I_p is the incident probe current, γ_A is the ionization probability, and η is the instrumental efficiency.

For our base pressure measurements on Al, we find that $\tau_{Al}=4.2\times10^{-4}$ and estimate $\eta=0.01$, so that the ionization probability at this pressure is $\gamma_{Al}=0.042$ which compares reasonably to a previously measured[19] unoxygenated probability of 0.01.

An important trend that Table III shows is that in order to increase the useful yield, an oxygen jet in this study was better than iodine, even though the practical sensitivity is usually higher with iodine (Table II). Table III also shows the ionization enhancement and the ratio of ionization enhancement to sputter enhancement. Iodine significantly enhances the sputter yield, and hence the sputter rate, while oxygen has little effect on the sputter yield it has a large effect on the ionization yield. Since it is the ratio of these yields that is important, here the increase of ionization yield due to oxygen wins out. We should stress that the geometry we used for iodine delivery was nonoptimal. Previous studies indicate that maximal sputter enhancement occurs for fluxes delivered closer to and more steeply inclined to the sample than physical limitations allowed in this study. We are in the process of modifying the system to allow this measurement in the future. From Table III we might estimate that increased useful yields for Ti, Mo, and W oxygen will be superior, and that for Al and Si, an optimized iodine system would be superior.

It should be noted that the use of iodine significantly reduces redeposition. For cases where sample volumes are not a major limitation, such as in depth profiling in a semiconductor, iodine makes the interpretation of the depth profile easier because of the increased practical sensitivity and the decreased redeposition. However, for samples which are volume limited, such as a small particle, an increased useful yield may be most important to obtain a SIMS spectrum or map, and oxygen should be used for enhancement. Depending on the task, either oxygen or iodine can be used to increase the effectiveness of FIB/SIMS for analytical work.

V. APPLICATIONS

We show three applications of FIB/SIMS to semiconductors. Mass spectra are useful for surveying areas for contamination, and as a first step sometimes for depth profiling and mapping.

Figure 4 shows a mass spectrum of a crater in an IC, an

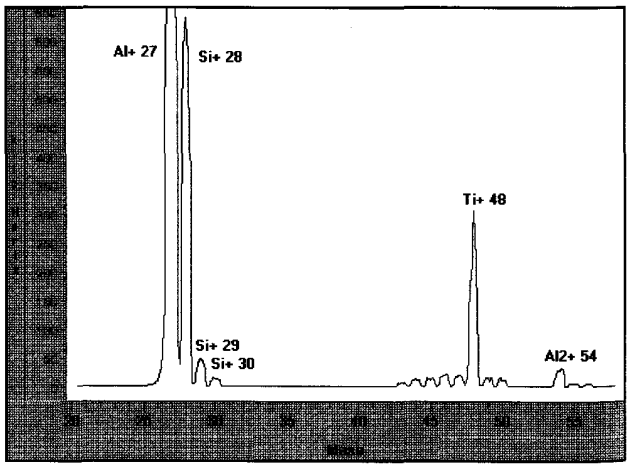

FIG. 4. Mass spectrum in the sputter crater of an IC. The field of view was 10 μm$\times$10 μm.

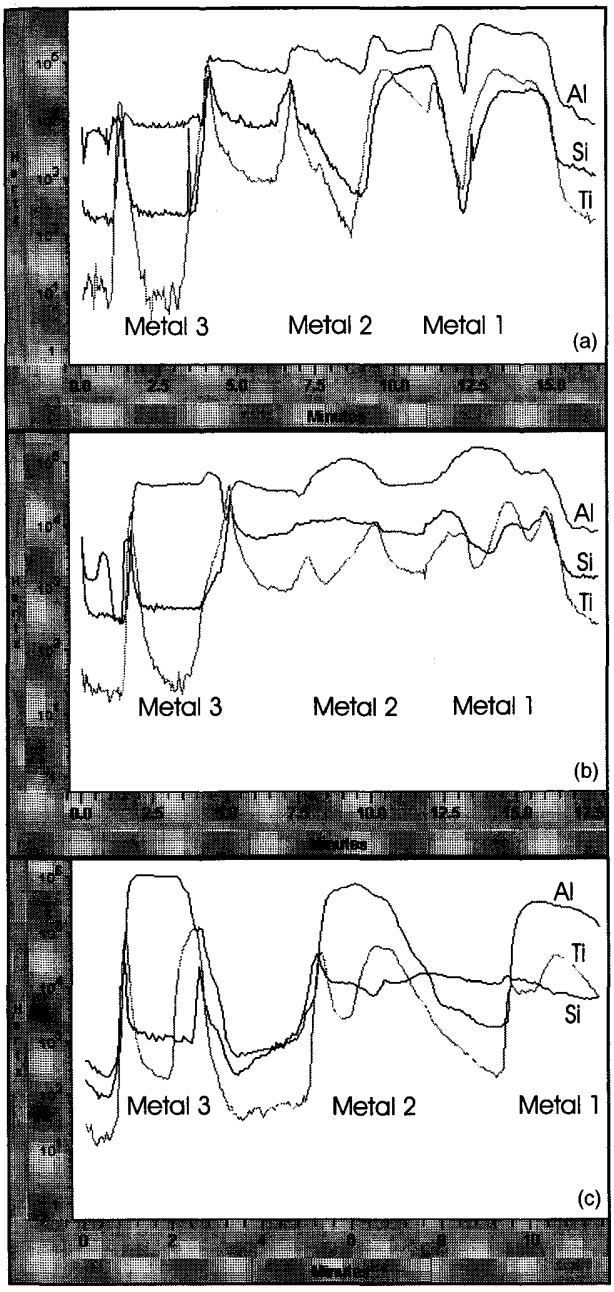

FIG. 5. Depth profile in an IC (a) $\leq 1\times10^{-7}$ Torr, (b) 5×10^{-5} Torr, (c) iodine flux introduced.

illustration of a quick survey. The mass resolution is <1 amu.

Depth profiles are essentially one-dimensional maps where time is depth. This is one reason why accurate sputter rates for materials are needed. Figures 5(a)–5(c) show a depth profiles in an IC. Clearly there are differences in the ease of interpretation of the spectra. In Fig. 5(c), the iodine flux was not optimized, but it shows that there is increased ionization, and that edge effects are apparently reduced. The nominal thickness of the Al metal layers are 1 μm (M3), 0.7 μm (M2), and 0.45 μm (M1).

Two-dimensional chemical maps utilize the high lateral spatial resolution of the FIB. Figure 6 shows a FIB secondary electron image and three elemental maps from a cross-sectioned IC. The images can be pseudocolored and overlayed to give accurate spatial relationships between the mapped species.

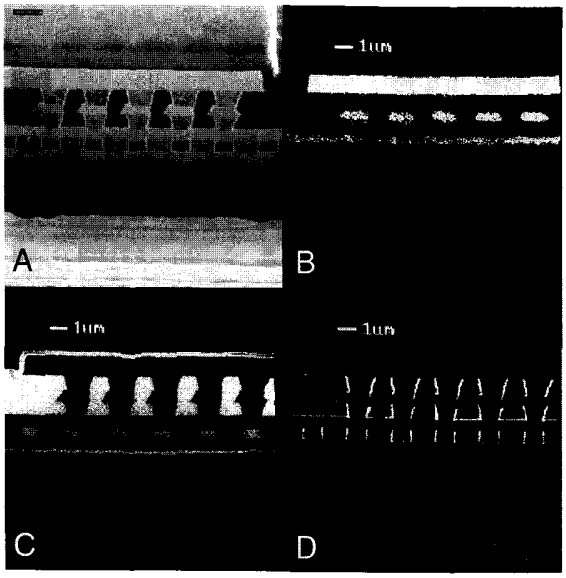

FIG. 6. Chemical map of a cross-sectioned face of an IC. (A) FIB secondary electron image. (B) Mass 27 Al. (C) Mass 28 (Si). (D) Mass 48 (Ti). The maps are 256×256 pixels. Primary beam current=40 pA.

VI. CONCLUSIONS

In order for FIB/SIMS to be better utilized in the semiconductor industry, more knowledge is needed to better interpret results. We have shown that it is possible to measure sputter yields and rates, to estimate the instrument efficiency, and that our measured useful yields and practical sensitivities show that FIB/SIMS is capable of attacking a variety of analysis challenges. We have found that there is an increase in the useful yield when either oxygen or iodine is introduced into the system. At present, it appears that the oxygen increases the useful yield more, and iodine increases practical sensitivity. More data is needed, especially for matrix effects and nonelemental materials.

ACKNOWLEDGMENTS

The contributions of a large number of people to the development of this FIB/SIMS and to measurements in this study are recognized: C. Bickford for electronics, D. Do for software, and R. Gerlach and M. Scheinfein for the optics and mechanical design. We thank J. Lenti and C. Doss for their superb AFM measurements. We thank L. Swanson for useful discussions throughout. One of us (M. U.) acknowledges the invaluable support of a Murdock Charitable Trust grant to the University of Portland.

[1]R. J. Young, Vacuum **44**, 353 (1993).
[2]E. C. G. Kirk, D. A. Williams, and H. Ahmed, Proc. Inst. Phys. Conf. **100**, 491 (1989).
[3]J. Puretz and L. W. Swanson, J. Vac. Sci. Technol. B **10**, 2695 (1992).

[4]K. Van Doorselaer, M. Van den Reeck, L. Van den Bempt, R. Young, and J. Whitney, ISTFA 1993: Proceedings of the 19th International Symposium for Testing and Failure Analysis, 1993 (unpublished), p. 405.
[5]R. Levi-Setti, Y. L. Wang, and G. Crow, J. Phys. (Paris) **45**, C9 (1984).
[6]R. Levi-Setti, J. M. Chabala, J. Li, K. L. Gavrilov, R. Mogilevski, and K. K. Soni, Scanning Microsc. **7**, 1161 (1993).
[7]R. Levi-Setti, J. M. Chabala, P. Hallegot, and Y. Wang, Microelectron. Eng. **9**, 391 (1989).
[8]G. A. Crow, Proceedings of the ISTFA 1991: The 17th International Symposium for Testing and Failure Analysis, 1992 (unpublished), pp. 401–407.
[9]J. A. McHugh, *Methods for Surface Analysis* (Elsevier, New York, 1975), p. 273.
[10]A. Benninghoven, F. G. Rudenauer, and H. W. Werner, *Secondary Ion Mass Spectrometry* (Wiley, New York, 1987).
[11]A. Leslie, Proceedings of the 5th European Symposium on Reliability of Electron Devices, Failure Physics and Analysis, 1994 (unpublished), p. 43.
[12]FEI Co., 7451 N. E. Evergreen Pkwy., Hillsboro, OR 97124.
[13]R. L. Gerlach, M. Scheinfein, G. Crow, M. Utlaut, and C. Bickford, Proc. SPIE **2014**, 149 (1993).
[14]Charged-particle optics simulation program from EG&G Idaho Inc., Idaho Falls, ID 83415.
[15]Model No. 7-324-9. Extrel Corp. 575 Epsilon Dr., Pittsburg, PA 15238.
[16]Dimension 5000 SPM, Digital Instruments, Santa Barbara, CA 93103.
[17]Model ARIS 3300 with AFM head, Burliegh Instruments Inc., Fishers, NY 14453.
[18]S. Somekh and H. C. Casey, Jr., Appl. Opt. **16**, 126 (1977).
[19]H. Werner, Surf. Sci. **49**, 301 (1975).